

## Accepted Manuscript

Synthesis, structure and *in vitro* biological activity of pyridoxal N(4)-substituted thiosemicarbazone cobalt(III) complexes

Rajendran Manikandan, Paranthaman Vijayan, Panneerselvam Anitha, Govindan Prakash, Periasamy Viswanathamurthi, Ray Jay Butcher, Krishnaswamy Velmurugan, Raju Nandhakumar

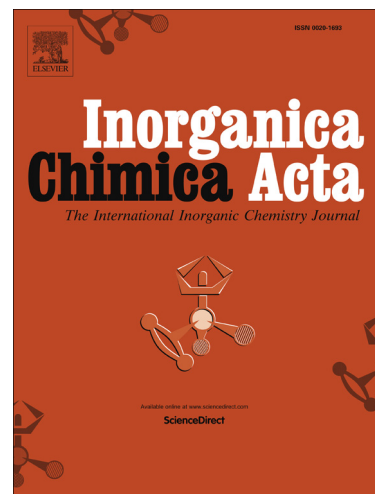
PII: S0020-1693(14)00327-2  
DOI: <http://dx.doi.org/10.1016/j.ica.2014.05.035>  
Reference: ICA 16017

To appear in: *Inorganica Chimica Acta*

Received Date: 18 April 2014  
Revised Date: 29 May 2014  
Accepted Date: 30 May 2014

Please cite this article as: R. Manikandan, P. Vijayan, P. Anitha, G. Prakash, P. Viswanathamurthi, R.J. Butcher, K. Velmurugan, R. Nandhakumar, Synthesis, structure and *in vitro* biological activity of pyridoxal N(4)-substituted thiosemicarbazone cobalt(III) complexes, *Inorganica Chimica Acta* (2014), doi: <http://dx.doi.org/10.1016/j.ica.2014.05.035>

This is a PDF file of an unedited manuscript that has been accepted for publication. As a service to our customers we are providing this early version of the manuscript. The manuscript will undergo copyediting, typesetting, and review of the resulting proof before it is published in its final form. Please note that during the production process errors may be discovered which could affect the content, and all legal disclaimers that apply to the journal pertain.



**Synthesis, structure and *in vitro* biological activity of pyridoxal N(4)-substituted thiosemicarbazone cobalt(III) complexes**

Rajendran Manikandan<sup>a</sup>, Paranthaman Vijayan<sup>a</sup>, Panneerselvam Anitha<sup>a</sup>, Govindan Prakash<sup>a</sup>, Periasamy Viswanathamurthi<sup>a,\*</sup>, Ray Jay Butcher<sup>b</sup>, Krishnaswamy Velmurugan<sup>c</sup>, Raju Nandhakumar<sup>c</sup>

<sup>a</sup>*Department of Chemistry, Periyar University, Salem-636 011, Tamil Nadu, India.*

<sup>b</sup>*Department of Chemistry, Howard University, 525 College Street NW, Washington, DC 20059, USA.*

<sup>c</sup>*Department of Chemistry, Karunya University, Karunya Nagar, Coimbatore - 641 114, India.*

\* Corresponding author. Fax: +91 427 2345124.

E-mail address: viswanathamurthi72@gmail.com (P. Viswanathamurthi).

**Abstract**

Cobalt(III) complexes containing pyridoxal N(4)-substituted thiosemicarbazone ligands with the composition  $[\text{Co}(\text{HL}^{1-2}.\text{Cl})(\text{HL}^{1-2}.\text{H}_2\text{O})]$  (**1-2**) have been synthesized from the reaction of  $[\text{CoCl}_2(\text{PPh}_3)_2]$  and pyridoxal N-methyl-thiosemicarbazone hydrochloride ( $\text{H}_3\text{L}^1.\text{Cl}$ )/pyridoxal N-phenyl-thiosemicarbazone hydrochloride ( $\text{H}_3\text{L}^2.\text{Cl}$ ). The richness of the coordination chemistry of this ligand is highlighted by the modulation of its charge from neutral ( $\text{H}_3\text{L}.\text{Cl}$ ) (L) to dianionic ( $\text{HL}.\text{Cl}$ ) ( $\text{L}^{2-}$ ) and monoanionic forms ( $\text{HL}.\text{H}_2\text{O}$ ) ( $\text{L}^-$ ) and coordinated as tridentate binegative mode around cobalt(III) ion by forming neutral complex. The new complexes were characterized by various analytical and spectroscopic techniques (IR, electronic,  $^1\text{H-NMR}$  and ESI-Mass). The X-ray crystal structure of the complex **2**, demonstrated distorted octahedral coordination geometry around the metal centre. Further, the investigation of effect of substitution ( $\text{CH}_3$  or  $\text{C}_6\text{H}_5$ ) on terminal N(4)-nitrogen of thiosemicarbazone exhibited its influence on the potential binding and cleavage ability with DNA, BSA binding, free radical scavenging and cytotoxicity.

**Keywords:** Cobalt(III) complexes; DNA interaction; Protein binding; Antioxidant; Cytotoxicity.

## 1. Introduction

Schiff base compounds are strong chelators obtained from the efficient condensation of aldehydes with amines. Metal complexes of these chelate ligands have variety of potential applications in diverse areas like medicine, agriculture, analytical chemistry, catalysis, enzyme modeling, magneto-structural chemistry, miscellaneous studies, dye and polymer industry etc. Aromatic Schiff bases derived from pyridine carbaldehyde and thiosemicarbazides exhibit admirable yield with high purity compared to their aliphatic counterpart, mainly because of the elevated strength and stability of their imine bonds conferred by the electron-rich pyridinyl side groups. In aromatic Schiff bases, pyridoxal based ones and especially, their metal complexes have drawn special interest in the past few decades due to their powerful antitumor activities [1, 2].

Previous reports on metal complexes of pyridoxal thiosemicarbazone ligands always suggests a terdentate binding mode via the S, N (iminic) and O (phenolic) donor atoms (Fig. 1a-b). Different types of stoichiometry are observed for this binding mode depending on the nature of the inorganic anion,  $M(H_2L)X_2$  ( $M = Mn, Cu$  or  $Zn$ ;  $X = Cl$  or  $NO_3$ ),  $M(HL)X$  ( $M = Co, Cu$  or  $Zn$ ;  $X = Cl$  or  $CH_3CO_2$ ),  $ML$  ( $M = Ni$  or  $Cu$ ; from acetate salts),  $[Co(HL)L]4.5H_2O$ ,  $[Co(HL)_2]ClEtOH$ ,  $[Ni(HL)py]NO_3$ ,  $[Ni(H_2L)_2](NO_3)_2 \cdot H_2O$ ,  $[MoO_2(HL)]Cl_n$ ,  $[Fe(HL)_2]X_n \cdot nH_2O$  ( $X = SO_4$  or  $NO_3$ ) and  $[Fe(HL)(L)] \cdot 8H_2O$  [3]. In some cases the coordination via phenolic-oxygen, imine-nitrogen and azomethine nitrogen atoms (Fig. 1c) [4] or through the hydroxymethyl group is also possible (Fig. 1d) [2]. In an  $Au^{III}$  complex, the ligand coordinates bidentately through the N and S-atoms of the thiosemicarbazide fragment (Fig. 1e) [5]. Unusual coordination of the  $HL^-$  anion to the metal only via its S-atom was also found in the pyridoxal thiosemicarbazonato complex of dimethylthallium(III) (Fig. 1f) [6]. As shown in Scheme 1, the ligand pyridoxal thiosemicarbazone can be found in different states from the neutral zwitterionic form L to the dianionic form  $L^{2-}$  and monoanionic form  $L^-$ .

<Insert Figure 1 and Scheme 1>

Cobalt is an element of biological attention and its role is mainly focused on its presence in the active center of vitamin B12, which regulates indirectly the synthesis of DNA [7]. Additionally, cobalt is an essential element present in co-enzyme of vitamin B12 and which is used as a supplement of the vitamin [8] and at least eight cobalt dependent proteins have been reported [7]. So far since the first reported studies on the biological activity of Co complexes [9] in 1952, diverse structurally characterized cobalt complexes have been studied as hydrolytic agents for DNA cleavage [10] and others showing antitumor-antiproliferative

[11-13], antimicrobial [14-16], antifungal [17,18], antiviral [19,20] and antioxidant [21,22] activity have been reported. For the last decade, our group has been actively engaged in the synthesis and characterization of N(4)-substituted thiosemicarbazone complexes with various transition metals and studied their applications [23]. In the continuation of our efforts in understanding the coordination propensities of pyridoxal N(4)-substituted thiosemicarbazones, we have carried out the structural characterization of new cobalt(III) complexes containing pyridoxal N(4)-substituted thiosemicarbazones ( $H_3L^{1-2}.Cl$ ) and tested their cytotoxicity on human breast carcinoma (MCF-7) and human cervix carcinoma (HeLa) tumor cell lines. Hence, in this paper, we are reporting the synthesis, characterization, crystallography, DNA binding/cleavage, protein binding ability and cytotoxic activities of new Co(III) pyridoxal N(4)-substituted thiosemicarbazone complexes.

## 2. Experimental

### 2.1. Materials and methods

All the reagents used were chemically pure and AR grade. The solvents were purified and dried according to standard procedures.  $CoCl_2 \cdot 6H_2O$ , calf-thymus DNA (CT-DNA), methylene blue (MB) and bovine serum albumin (BSA) were purchased from Sigma-Aldrich and used as received. The pBR322 DNA was purchased from Bangalore GeNei, Bangalore, India. The human breast carcinoma cell line (MCF-7) and human cervix carcinoma cell line (HeLa) was obtained from National Centre for Cell Science (NCCS), Pune, India and grown in Dulbeccos Modified Eagles Medium (DMEM) containing 10% fetal bovine serum (FBS). Cells were maintained at  $37^\circ C$ , 5%  $CO_2$ , 95% air and 100% relative humidity. Maintenance cultures were passaged weekly, and the culture medium was changed twice a week.

### 2.2. Physical measurements

Microanalyses of carbon, hydrogen, nitrogen and sulfur were carried out using Vario EL III Elemental analyzer at SAIF – Cochin, India. The IR spectra of the ligand and their complexes were obtained as KBr pellets on a Nicolet Avatar model spectrophotometer at  $4000 - 400\text{ cm}^{-1}$  range. Electronic spectra of the ligand and their complexes have been recorded in methanol using a Shimadzu UV - 1650 PC spectrophotometer at  $800 - 200\text{ nm}$  range. Emission spectra were measured with a Jasco FP 6600 spectrofluorometer.  $^1H$ -NMR spectra were recorded in Jeol GSX - 300 instrument at room temperature using tetramethylsilane as the internal standard in dimethylsulfoxide ( $DMSO-d_6$ ) as solvent. The

ESI-MS spectra were recorded by LC-MS Q-ToF Micro analyzer (Shimadzu) in the SAIF, Punjab University, Chandigarh. Melting points were checked on a Technico micro heating table and are uncorrected. The requisite precursor metal complex  $[\text{CoCl}_2(\text{PPh}_3)_2]$  were prepared according to the literature method [24].

### 2.3. Preparation pyridoxal thiosemicarbazone hydrochloride ligands

The synthetic routes for ligands ( $\text{H}_3\text{L}^{1-2}\cdot\text{Cl}$ ) are presented in Scheme 2. Pyridoxal N(4)-substituted thiosemicarbazone hydrochloride has been prepared according to a modification of the procedure described in the literature [25]. Substituted thiosemicarbazide (2 mmol) was dissolved in 10 mL of ethanol with constant stirring, and was added to pyridoxal hydrochloride (2 mmol) dissolved in 10 mL of ethanol. The mixture was stirred at 80 °C for 30 min. After the reaction mixture was cooled to room temperature, the yellow solid was isolated by filtration, washed with ethanol and dried in *vacuo*.

#### 2.3.1. Pyridoxal-4-methyl-thiosemicarbazone hydrochloride ( $\text{H}_3\text{L}^1\cdot\text{Cl}$ )

$\text{H}_3\text{L}^1\cdot\text{Cl}$  was prepared from the reaction of pyridoxal hydrochloride (0.4072 g; 2 mmol) and 4-methyl-thiosemicarbazide (0.2103 g; 2 mmol). Yield: 0.4245 g, 73%; Colour: yellow solid; M. p.: 226 °C; Anal. Calc. for  $\text{C}_{10}\text{H}_{15}\text{ClN}_4\text{O}_2\text{S}$  (290.77 g,  $\text{mol}^{-1}$ ): C, 41.30; H, 5.19; N, 19.26; S, 11.02%. Found: C, 41.12; H, 5.36; N, 19.57; S, 10.88%. IR (KBr,  $\text{cm}^{-1}$ ): 3380(m)  $\nu(\text{CH}_2\text{OH})$ , 3300(m)  $\nu(-\text{NH}-\text{R})$ , 3200(s)  $\nu(\text{OH})$ , 3152(m)  $\nu(\text{NH})$ , 2706(m)  $\nu(\text{NH}^+)$ , 1615(s)  $\nu(\text{C}=\text{N})$ , 830(s)  $\nu(\text{C}=\text{S})$ . UV-Vis ( $\text{CH}_3\text{OH}$ ,  $\lambda/\text{nm}$  ( $\epsilon/\text{M}^{-1}\text{cm}^{-1}$ )): 230 (11 467), 338 (11 567).  $^1\text{H}$  NMR (300 MHz,  $\text{DMSO}-d_6$ ,  $\delta$ , ppm): 12.17 (s, 1H, OH), 8.93 (s, 1H, NH), 8.65 (s, 1H, NH-R), 8.52 (s, 1H, CH=N), 8.17 (s, 1H, Py), 5.39 (s, 1H, OH), 4.78 (s, 2H,  $\text{CH}_2$ ), 3.02 (s, 3H,  $\text{CH}_3$ ), 2.62 (s, 3H,  $\text{CH}_3$ ).

#### 2.3.2. Pyridoxal-4-phenyl-thiosemicarbazone hydrochloride ( $\text{H}_3\text{L}^2\cdot\text{Cl}$ )

$\text{H}_3\text{L}^2\cdot\text{Cl}$  was prepared from the reaction of pyridoxal hydrochloride (0.4072 g; 2 mmol) and 4-phenyl-thiosemicarbazide (0.3344 g; 2 mmol). Yield: 0.5645 g, 80%; Colour: yellow solid; M. p.: 226 °C; Anal. Calc. for  $\text{C}_{15}\text{H}_{17}\text{ClN}_4\text{O}_2\text{S}$  (352.84 g,  $\text{mol}^{-1}$ ): C, 51.06; H, 4.85; N, 15.87; S, 9.08%. Found: C, 50.79; H, 4.73; N, 15.58; S, 9.42%. IR (KBr,  $\text{cm}^{-1}$ ): 3388(s)  $\nu(\text{CH}_2\text{OH})$ , 3360(m)  $\nu(-\text{NH}-\text{R})$ , 3240  $\nu(\text{OH})$ , 3157(m)  $\nu(\text{NH})$ , 2822(m)  $\nu(\text{NH}^+)$ , 1640(s)  $\nu(\text{C}=\text{N})$ , 860(m)  $\nu(\text{C}=\text{S})$ . UV-Vis ( $\text{CH}_3\text{OH}$ ,  $\lambda/\text{nm}$  ( $\epsilon/\text{M}^{-1}\text{cm}^{-1}$ )): 233 (31 547), 324 (36 671), 349 (35 568).  $^1\text{H}$  NMR (300 MHz,  $\text{DMSO}-d_6$ ,  $\delta$ , ppm): 11.58 (s, 1H, OH), 9.97 (s, 1H, NH), 8.90 (s, 1H, NH-

R), 8.40 (s, 1H, CH=N), 7.52-7.75 (m, 5H, Ph), 6.97 (s, 1H, Py), 5.38 (s, 1H, OH), 4.78 (s, 2H, CH<sub>2</sub>), 1.56 (s, 3H, CH<sub>3</sub>).

#### 2.4. Synthesis of cobalt(III) complexes

All the new metal complexes were prepared according to the following general procedure. A warm ethanol solution (10 mL) containing H<sub>3</sub>L<sup>1-2</sup>.Cl (1 mmol) was added to ethanol solution (10 mL) of [CoCl<sub>2</sub>(PPh<sub>3</sub>)<sub>2</sub>] (1 mmol). The resulting reddish solution was refluxed for 5 h. Dark red coloured crystalline powder was obtained on slow evaporation. They were filtered off, washed with cold ethanol, and dried under *vacuo*.

##### 2.4.1. Synthesis of [Co(HL<sup>1</sup>.Cl)(HL<sup>1</sup>.H<sub>2</sub>O)] (1)

The complex was synthesized from [CoCl<sub>2</sub>(PPh<sub>3</sub>)<sub>2</sub>] (0.654 g; 1 mmol) and H<sub>3</sub>L<sup>1</sup>.Cl (0.2907 g; 1 mmol). Yield: 0.4456 g, 72%; Colour: red solid; M.p.: 172 °C; Anal. calcd for C<sub>20</sub>H<sub>28</sub>ClCoN<sub>8</sub>O<sub>5</sub>S<sub>2</sub> (619.00 g, mol<sup>-1</sup>): C, 38.81; H, 4.56; N, 18.10; S, 10.36%. Found: C, 38.53; H, 4.86; N, 18.49; S, 10.62%. IR (KBr, cm<sup>-1</sup>): 3422(b) ν(H<sub>2</sub>O), 3391(m) ν(CH<sub>2</sub>OH), 3286(s) ν(-NH-R), 2776(m) ν(NH<sup>+</sup>), 1611(s) ν(C=N), 1580(s) ν(C=N), 755(s) ν(C-S). UV-Vis (CH<sub>3</sub>OH, λ/nm (ε/M<sup>-1</sup> cm<sup>-1</sup>)): 223 (21 5711), 254 (15 1373), 358 (53 094), 438 (44 870) <sup>1</sup>H NMR (300 MHz, DMSO-d<sub>6</sub>, δ, ppm): 8.69 (s, 1H, NH-R), 8.53 (s, 1H, CH=N), 7.60 (s, 1H, Py), 5.29 (s, 1H, OH), 4.72 (s, 2H, CH<sub>2</sub>), 2.86 (s, 3H, CH<sub>3</sub>), 2.16 (s, 3H, CH<sub>3</sub>). ESI-MS, *m/z* (%): 565.0 (57) [M-Cl.H<sub>2</sub>O]<sup>+</sup>.

##### 2.4.2. Synthesis of [Co(HL<sup>2</sup>.Cl)(HL<sup>2</sup>.H<sub>2</sub>O)] (2)

The complex was synthesized from [CoCl<sub>2</sub>(PPh<sub>3</sub>)<sub>2</sub>] (0.654 g; 1 mmol) and H<sub>3</sub>L<sup>2</sup>.Cl (0.3528 g; 1 mmol). Single crystals suitable for X-ray diffraction were grown at room temperature from ethanol. Yield: 0.6019 g, 81%; Colour: red solid; M.p.: 196 °C; Anal. calcd for C<sub>30</sub>H<sub>32</sub>ClCoN<sub>8</sub>O<sub>5</sub>S<sub>2</sub> (743.14 g, mol<sup>-1</sup>): C, 48.49; H, 4.34; N, 15.08; S, 8.63%. Found: C, 48.74; H, 4.66; N, 15.57; S, 8.42%. IR (KBr, cm<sup>-1</sup>): 3420(b) ν(H<sub>2</sub>O), 3396(m) ν(CH<sub>2</sub>OH), 3370(s) ν(-NH-R), 2751(s) ν(NH<sup>+</sup>), 1600(s) ν(C=N), 1586(s) ν(C=N), 750(s) ν(C-S). UV-Vis (CH<sub>3</sub>OH, λ/nm (ε/M<sup>-1</sup> cm<sup>-1</sup>)): 225 (10 74740), 263 (91 6151), 372 (29 0074), 454 (23 8945). <sup>1</sup>H NMR (300 MHz, DMSO-d<sub>6</sub>, δ, ppm): 9.90 (s, 1H, NH-R), 8.85 (s, 1H, CH=N), 7.55-7.78 (m, 5H, Ph), 6.98 (s, 1H, Py), 5.28 (s, 1H, OH), 4.78 (s, 2H, CH<sub>2</sub>), 2.16 (s, 3H, CH<sub>3</sub>). ESI-MS, *m/z* (%): 689.1 (68) [M-Cl.H<sub>2</sub>O]<sup>+</sup>.

## 2.5. X-ray Crystallography

Crystal data were collected on an Oxford/Agilent Gemini diffractometer. Structures were solved using the direct methods program SHELXL [26]. All nonsolvent heavy atoms were located using subsequent difference Fourier syntheses. The structures were refined against F<sup>2</sup> with the program SHELXL [27], in which all data collected were used including negative intensities. All nonsolvent heavy atoms were refined anisotropically. All nonsolvent hydrogen atoms were idealized using the standard SHELXL idealization methods.

## 2.6. DNA binding and cleavage experiments

Luminescence measurement was performed to clarify the binding affinity of cobalt(III) complexes by emissive titration at room temperature. The complexes were dissolved in mixed solvent of 5% DMSO and 95% Tris-HCl buffer (5 mM Tris-HCl/50 mM NaCl buffer for pH = 7.2) for all the experiments and stored at 4 °C for further use and used within 4 days. Tris-HCl buffer was subtracted through base line correction. The excitation wavelength was fixed by the emission range and adjusted before measurements. Emissive titration experiments were performed with a fixed concentration of metal complexes (25 μM). While gradually increasing the concentration of DNA (0 - 25 μM), the emission spectra were monitored by keeping the excitation of the test compounds at 400 nm. MB-DNA experiments were conducted by adding the complexes to the Tris-HCl buffer of MB-DNA. The change in the fluorescence intensity was recorded. The excitation and emission wavelengths were 605 and 684 nm, respectively.

DNA cleavage experiments were carried out according to reported procedure [28]. For the gel electrophoresis experiment, supercoiled pBR322 DNA was treated with the cobalt(III) complexes in TEA buffer (10 mM Tris acetate, 10 mM EDTA, pH = 8.0) and the solution was then incubated at 37 °C for 2 h. Loaded 20 μL of DNA sample (mixed with bromophenol blue dye, 1:1 ratio), carefully into the wells, along with standard DNA marker. The samples were analyzed by electrophoresis for 30 min at 50 V on a 0.8% agarose gel in TEA (4.84 g Tris-acetate, 0.5 mol EDTA/1 L, pH = 8.0). The gel was stained with 10 μg/mL ethidium bromide and observed the bands under illuminator.

## 2.7. Protein binding

The excitation wavelength of BSA at 280 nm and the emission at 344 nm were monitored for the protein binding studies. The excitation and emission slit widths and scan rates were

maintained constant for all of the experiments. A stock solution of BSA was prepared in 5 mM Tris-HCl/50 mM NaCl buffer (pH = 7.2) and stored in the dark at 4 °C for further use. The concentrated stock solutions of the complexes were prepared as mentioned for the DNA binding experiments, except that the phosphate buffer was used instead of a Tris-HCl buffer for all of the experiments. Titrations were manually done by a micropipet for the addition of the complexes.

## 2.8. Antioxidant assays

### 2.8.1. DPPH<sup>•</sup> scavenging assay

The 2,2-diphenyl-1-picrylhydrazyl (DPPH) radical scavenging activity of the compounds was measured according to the method of Blios [29]. The DPPH radical is a stable free radical. Because of the odd electron, DPPH shows a strong absorption band at 517 nm in the visible spectrum. As this electron becomes paired off in the presence of a free radical scavenger, the absorption vanishes and the resulting decolorization is stoichiometric with respect to the number of electrons taken up. Various concentrations of the experimental complexes were taken and the volume was adjusted to 100  $\mu$ L with methanol. About 5 mL of a 0.1 mM methanolic solution of DPPH was added to the aliquots of samples and standards (BHT and vitamin C) and shaken vigorously. A negative control was prepared by adding 100  $\mu$ L of methanol in 5 mL of 0.1 mM methanolic solution of DPPH. The tubes were allowed to stand for 20 min at 27 °C. The absorbance of the sample was measured at 517 nm against the blank (methanol).

### 2.8.2. OH<sup>•</sup> scavenging assay

The hydroxyl radical scavenging activity of the compounds has been investigated by using the Nash method [30]. *In vitro* hydroxyl radicals were generated by an Fe<sup>3+</sup>/ascorbic acid system. The detection of hydroxyl radicals was carried out by measuring the amount of formaldehyde formed from the oxidation reaction with DMSO. The formaldehyde produced was detected spectrophotometrically at 412 nm. A mixture of 1.0 mL of iron-EDTA solution (0.13% ferrous ammonium sulphate and 0.26% EDTA), 0.5 mL of EDTA solution (0.018%), and 1.0 mL of DMSO (0.85% DMSO (v/v) in 0.1 M phosphate buffer, pH 7.4) were sequentially added in the test tubes. The reaction was initiated by adding 0.5 mL of ascorbic acid (0.22%) and was incubated at 80–90 °C for 15 min in a water bath. After incubation, the

reaction was terminated by the addition of 1.0 mL of ice-cold trichloroacetic acid (17.5% w/v). Subsequently, 3.0 mL of Nash reagent was added to each tube and left at room temperature for 15 min. The intensity of the colour formed was measured spectrophotometrically at 412 nm against the reagent blank.

### 2.8.3. NO scavenging assay

The assay of nitric oxide (NO) scavenging activity is based on a method [31] where sodium nitroprusside in aqueous solution at physiological pH spontaneously generates nitric oxide, which interacts with oxygen to produce nitrite ions. These can be estimated using the Griess reagent. Scavengers of nitric oxide compete with oxygen leading to less production of nitrite ions. For the experiment, sodium nitroprusside (10 mM) in phosphate buffered saline was mixed with a fixed concentration of the complex and standards were incubated at room temperature for 150 min. After the incubation period, 0.5 mL of Griess reagent containing 1% sulfanilamide, 2% H<sub>3</sub>PO<sub>4</sub> and 0.1% *N*-(1-naphthyl) ethylenediamine dihydrochloride were added. The absorbance of the chromophore formed was measured at 546 nm.

### 2.9. *In vitro* cytotoxic activity evaluation by MTT assays

Standard 3-(4,5-dimethylthiazole)-2,5-diphenyltetraazolium bromide (MTT) assay procedures were used [32]. The monolayer cells were detached with trypsin-ethylenediaminetetraacetic acid (EDTA) to make single cell suspensions and viable cells were counted using a hemocytometer and diluted with medium containing 5% FBS to give final density of  $1 \times 10^5$  cells/mL. One hundred microlitres per well of cell suspension were seeded into 96-well plates at plating density of 10,000 cells/well and incubated to allow for cell attachment at 37 °C, 5% CO<sub>2</sub>, 95% air and 100% relative humidity. After 24 h the cells were treated with serial concentrations of the test samples. They were initially dissolved in neat dimethylsulfoxide (DMSO) to prepare the stock (200 mM) and stored frozen prior to use. At the time of drug addition, the frozen concentrate was thawed and an aliquot was diluted to twice the desired final maximum test concentration with serum free medium. Additional three, 10 fold serial dilutions were made to provide a total of four drug concentrations. Aliquots of 100  $\mu$ L of these different drug dilutions were added to the appropriate wells already containing 100  $\mu$ L of medium, resulted the required final drug concentrations. Following drug addition the plates were incubated for an additional 48 h at 37

°C, 5% CO<sub>2</sub>, 95% air and 100% relative humidity. The medium containing without samples were served as control and triplicate were maintained for all concentrations.

MTT is a yellow water soluble tetrazolium salt. A mitochondrial enzyme in living cells, succinate-dehydrogenase, cleaves the tetrazolium ring, converting the MTT to an insoluble purple formazan. Therefore, the amount of formazan produced is directly proportional to the number of viable cells. After 48 h of incubation, 15 µL of MTT (5 mg/mL) in phosphate buffered saline (PBS) was added to each well and incubated at 37 °C for 4 h. The medium with MTT was then flicked off and the formed formazan crystals were solubilized in 100 µL of DMSO and then measured the absorbance at 570 nm using a micro plate reader. The % cell inhibition was determined using the following formula. % cell Inhibition = 100 - Abs (sample)/Abs (control) x 100. Nonlinear regression graph was plotted between % Cell inhibition and Log<sub>10</sub> concentration and IC<sub>50</sub> was determined using GraphPad Prism software.

### 3. Results and Discussion

Reaction in warm ethanol solution of H<sub>3</sub>L<sup>1-2</sup>.Cl and [CoCl<sub>2</sub>(PPh<sub>3</sub>)<sub>2</sub>] in 1:1 molar ratio (Scheme 2) with the following expectations that these pyridoxal N(4)-substituted thiosemicarbazones could behave as

<Insert Scheme 2>

- (i) A binegative tridentate ONS chelating system to yield a four coordinated complex (product 1), or
- (ii) A uninegative tridentate chelating system through ONS donor atoms to form yet another type of four coordinated complex (product 2).

Unexpectedly, the pyridoxal N(4)-substituted thiosemicarbazone ligands (H<sub>3</sub>L<sup>1-2</sup>.Cl) involved in this work deceived all our expectations and formed stable six coordinated metal chelates with 1:2 metal–ligand stoichiometry (product 3), yielded the red bis ligand complexes of the general formula [Co(HL<sup>1-2</sup>.Cl)(HL<sup>1-2</sup>.H<sub>2</sub>O)] (**1-2**) (Scheme 2). The isolated complexes are crystalline powder that are stable in air, in addition to being soluble in common organic solvents such as dichloromethane, chloroform, benzene, acetonitrile, ethanol, methanol, dimethylformamide, DMSO and also soluble in water. All the new complexes were structurally characterized by elemental analyses, IR, electronic, <sup>1</sup>H NMR and ESI-Mass spectra. In addition single crystals of complex **2**, used to determine its molecular structure by X-ray crystallographic analysis, which is shown in Fig. 2.

### 3.1. IR spectra

IR spectroscopy has been used in order to confirm the bideprotonation and binding mode of pyridoxal N(4)-substituted thiosemicarbazones and identify the tautomeric as well as the ionic form of pyridoxal thiosemicarbazones in the solid state (Figs. S1-S4, Supporting information). Evidence of the solid compound being the HCl adduct appears from the IR spectrum in which a band at 2706-2822  $\text{cm}^{-1}$  could be addressed as the  $\nu(\text{N-H}^+ \text{Cl}^-)$  stretching vibration confirming that the nitrogen atom of the pyridine ring bears a proton [33]. There is no peak observed around 2500  $\text{cm}^{-1}$  assignable to the SH group; absorptions attributed at 830-860  $\text{cm}^{-1}$  which could be assigned to the  $\nu(\text{C=S})$  vibration of the free ligand indicating that it is present in the thione form. This band completely disappeared in the complexes, and two new bands appeared at 1580-1586  $\text{cm}^{-1}$  and 750-755  $\text{cm}^{-1}$  corresponding to a possible  $\nu(\text{C=N-N=C})$  and  $\nu(\text{C-S})$  stretching vibrations respectively, indicating coordination of a thiolate sulfur atom after enolization followed by deprotonation. In the high-energy range there appears a strong and broad band with the maximum at 3380-3388  $\text{cm}^{-1}$  (ligand), i.e., at 3391-3396 (complexes) that can be unambiguously assigned to the  $\nu(\text{OH})$  (hydroxymethyl) vibration [34]. In addition, the new broad band appeared at 3420-3422  $\text{cm}^{-1}$  are assigned to pyridine ring  $\text{NH}^+$  adduct  $\text{H}_2\text{O}$  ( $\nu(\text{N-H}^+.\text{H}_2\text{O})$ ) in complexes. Further, the stretching vibrations of the  $\nu(\text{NHR})$  (aminic) group appear in the 3286-3370  $\text{cm}^{-1}$  region; while the  $\nu(\text{NH})$  (hydrazinic) band occurring at 3152-3157  $\text{cm}^{-1}$  in the free ligands disappears in the complexes, suggesting deprotonation of the  $-\text{NH}$  group [34]. Coordination of the phenolate group is indicated by the disappearance of the OH stretching vibration as observed for the free ligands at 3200-3240  $\text{cm}^{-1}$  in the IR spectra of the complexes [25]. The free ligands showed a very strong absorption around 1615-1640  $\text{cm}^{-1}$  characteristic of the azomethine  $\nu(>\text{C=N})$  group. In all the complexes, the band due to azomethine was observed at a lower region around 1600-1611  $\text{cm}^{-1}$  indicating the coordination of azomethine nitrogen to cobalt.

### 3.2. Electronic spectra

The electronic spectral data for the investigated ligands and complexes in methanol, recorded in the range of 200–800 nm. As can be seen (Figs. S5-S8, Supporting information), the spectra display two to four electronic transitions. The strong peak at the blue end of the spectra of the compounds at 230 -324 nm can be ascribed to  $\pi-\pi^*$  pyridine and phenyl ring

absorptions [35]. The bands appeared in the region 338-372 nm have been assigned to  $n-\pi^*$  transitions of imine function of azomethine moiety. Metallation of ligands causes a red shift in these electronic transitions for complexes. Also the absorption band at 438-454 nm is attributed to ligand-to-metal charge transfer transitions (LMCT) [36].

### 3.3. $^1\text{H}$ NMR spectra

$^1\text{H}$  NMR spectroscopy has also been used in order to confirm the bideprotonation of the pyridoxal N(4)-substituted thiosemicarbazones and the stability of the complexes in solution (Figs. S9-S12, Supporting information). The  $^1\text{H}$  NMR spectra of the ligands showed a broad signal at  $\delta$  11.58-12.17 and 8.93-9.97 due to the phenolic OH and N–NH– protons, indicating their existence in the hydroxy-thione tautomeric form possessing a –NH–(C=S)–NHR moiety [37]. In the spectra of ligands, a singlet observed at  $\delta$  8.40-8.52 was assigned to azomethine proton and the signal appeared at  $\delta$  6.97-8.17 due to the aromatic pyridine proton [3(k)]. The presence of a singlet at  $\delta$  3.02 was assigned to N-methyl protons of  $\text{H}_3\text{L}^1\text{.Cl}$  ligand and multiplet appeared at  $\delta$  7.52-7.75 assignable to N-phenyl protons of the  $\text{H}_3\text{L}^2\text{.Cl}$  ligand. A sharp singlet at  $\delta$  8.65-8.90 confirmed the presence of terminal NH protons. The peak appeared at  $\delta$  1.56-2.62 has been assigned to methyl group. The methylene protons and aliphatic OH protons ( $\text{CH}_2\text{OH}$ ) appeared in the region at  $\delta$  4.78 and 5.38-5.39, respectively for all the ligands. The  $^1\text{H}$  NMR spectra of the complexes exhibited a sharp singlet at  $\delta$  8.53-8.85 and 8.69-9.90 corresponding to azomethine proton and terminal –NH protons of the thiosemicarbazone, respectively. A singlet which appeared at  $\delta$  6.98-7.60 in all the new complexes has been assigned to aromatic pyridine protons. The N-methyl group protons and N-phenyl group protons appeared in the region at  $\delta$  2.86 and 7.55-7.78, respectively. The methyl protons, methylene protons and aliphatic OH protons ( $\text{CH}_2\text{OH}$ ) also appeared in the corresponding region for all the complexes.

### 3.4. Mass Spectra

ESI-Mass spectral analyses of the new complexes were studied in order to confirm the molecular mass of the complexes (Figs. S13-S14, Supporting information). Complexes **1** and **2** showed an intense peak at  $m/z = 565.0$  and  $689.1$  respectively, due to the  $[\text{M-Cl.H}_2\text{O}]^+$  ion. The obtained molecular masses are in good agreement with that of the calculated molecular masses.

### 3.5. X-ray crystallography

Single-crystal X-ray analysis reveals that complex **2** crystallize in the triclinic system, with space group  $P2_1/c$ . Crystal details, crystallographic data, and refinement were summarized in Table 1. Selected bond lengths and bond angles have been reported in Table 2. The ORTEP view of the molecular structure with atom labelling scheme of the respective complex **2** without hydrogen atom has been shown in Fig. 2. The  $[\text{Co}(\text{HL}^3\cdot\text{Cl})(\text{HL}^3\cdot\text{H}_2\text{O})]$  unit contains a Co(III) ion in an distorted octahedral environment of  $\text{O}_2\text{N}_2\text{S}_2$  donor atoms from the two tridentate pyridoxalthiosemicarbazone ligands. The  $[\text{Co}(\text{O}_2\text{N}_2\text{S}_2)]$  coordination core consists of two oxygen atoms (phenolate), two nitrogen atoms (imine) in trans disposition, and two sulfur atoms. The binding of the ligands involve the formation of four metallocycles, comprised of two five-membered thiosemicarbazide S, N-chelate ring together with two six-membered pyridoxilydene N, O-chelate ring. Though the donor atoms and binding modes of the two ligands are same, they are not identical in nature. i.e, one ligand bound with metal as bianionic whiles the other as monoanionic and so the complex remains neutral with cobalt ion in 3+ oxidation state. Bianionic form (form II) of the ligand  $(\text{HL}^2\cdot\text{Cl})(\text{L}^{2-})$  has bound via deprotonated phenolic oxygen and thiolic sulphur formed in the rearrangement hydrazinic bonds. Pyridinium cation of this form has been satisfied by chloride ion and hence as the whole the ligand act as bianionic in nature. Monoanionic form (form III) of the ligand  $(\text{HL}^2\cdot\text{H}_2\text{O})(\text{L}^-)$  is similar with form II in binding modes, however the pyridinium ion has not been satisfied by negative ions and hence the ligand shows monoanionic nature. Nevertheless the pyridinium hydrogen create hydrogen bond with a water molecule (Scheme 1) which is evident from the crystal structure of complex **2**. The distances to the ligand donor atoms are  $\text{Co-S1A} = 2.2151(16)$  Å,  $\text{Co-S1B} = 2.1961(13)$  Å;  $\text{Co-O1A} = 1.911(4)$  Å,  $\text{Co-O1B} = 1.9273(13)$  Å; and  $\text{Co-N1A} = 1.914(4)$  Å,  $\text{Co-N1B} = 1.911(4)$  Å respectively and these values are equal to that of several cobalt(III) complexes previously noted [3(c)]. The angles around the Co center deviate significantly from  $90^\circ$ , the  $\text{N1B-Co-S1A}$  and  $\text{O1A-Co-N1A}$  angles have opened up to  $95.97$  and  $94.64^\circ$ , respectively and the  $\text{N1A-Co-S1A}$  and  $\text{O1A-Co-N1B}$  angles have reduced to  $86.97$  and,  $82.50^\circ$  indicating distortion from a regular octahedron [38, 39]. The packing of complex **2** is supported by intermolecular hydrogen bonding between the H-atom of water and the N(3)-atom of the hydrazinic group and Cl atom as well as between the oxygen atom of water and H-atom of the pyridinyl group N(2). The observed molecular conformation in complex **2** is stabilized by an intramolecular N-H...Cl and N-H...H<sub>2</sub>O interactions (Fig. 3).

&lt;Insert Figure 2 and 3&gt;

**Table 1**Crystal data and structure refinement for the complex **2**.

Complex	<b>2</b>
Empirical formula	C <sub>30</sub> H <sub>32</sub> ClCoN <sub>8</sub> O <sub>5</sub> S <sub>2</sub>
Formula weight	743.14
Colour	Red
Crystal dimensions (mm <sup>3</sup> )	0.3545x0.2683x0.2280
Temperature (K)	123(2)
Wavelength (Å)	1.54184
Crystal system	Monoclinic
Space group	<i>P</i> 2 <sub>1</sub> /c
Unit cell dimensions (Å, °)	<i>a</i> = 13.875(2) <i>b</i> = 17.8123(15) <i>c</i> = 13.7429(12) <i>β</i> = 105.122(12)
Volume Å <sup>3</sup>	3279.0(6)
<i>Z</i>	4
Calculated density (Mg/m <sup>3</sup> )	1.505
Absorption coefficient (mm <sup>-1</sup> )	6.490
<i>F</i> (000)	1536
Theta range for data collection (°)	3.30-74.16
Absorption correction	Analytical
Refinement method	Full-matrix least squares on <i>F</i> <sup>2</sup>
Data/restraints/parameters	6464 /3/413
Goodness-of-fit on <i>F</i> <sup>2</sup>	1.040
<i>R</i> indices [ <i>I</i> >2σ( <i>I</i> )]	<i>R</i> <sub>1</sub> = 0.0803, <i>wR</i> <sub>2</sub> = 0.1928
<i>R</i> indices (all data)	<i>R</i> <sub>1</sub> = 0.1136, <i>wR</i> <sub>2</sub> = 0.2286
Largest diff. peak and hole (e Å <sup>-3</sup> )	0.914 and -0.653

**Table 2**Selected bond lengths (Å) and angles (°) for the complex **2**.

Co-O(1A)	1.911(4)	O(1A)-Co-S(1A)	176.81(12)
Co-N(1A)	1.914(4)	O(1B)-Co-S(1B)	176.87(8)
Co-S(1A)	2.2151(16)	N(1B)-Co-N(1A)	176.58(19)
Co-O(1B)	1.9273(13)	O(1A)-Co-N(1A)	94.64(18)
Co-N(1B)	1.911(4)	N(1A)-Co-S(1A)	86.97(14)
Co-S(1B)	2.1961(13)	O(1A)-Co-S(1B)	90.61(11)
O(1A)-C(1A)	1.280(6)	O(1A)-Co-N(1B)	82.50(17)
N(1A)-N(3A)	1.369(6)	O(1A)-Co-O(1B)	89.78(12)
N(1A)-C(8A)	1.289(7)	N(1B)-Co-S(1A)	95.97(14)
S(1A)-C(9A)	1.752(6)	S(1B)-Co-S(1A)	92.12(6)
O(1B)-C(1B)	1.291(6)	N(1B)-Co-O(1B)	95.79(13)
N(1B)-N(3B)	1.387(5)	N(1A)-Co-O(1B)	86.06(13)
N(1B)-C(8B)	1.291(7)	N(1B)-Co-S(1B)	87.34(12)
S(1B)-C(9B)	1.751(5)	N(1A)-Co-S(1B)	90.81(13)
N(3A)-C(9A)	1.292(7)	O(1B)-Co-S(1A)	87.59(6)
N(4A)-C(9A)	1.378(7)		
N(3B)-C(9B)	1.285(7)		
N(4B)-C(9B)	1.372(6)		
N(2A)-H(2AA)	0.8800		
N(2B)-H(2BA)	0.8800		

### 3.6. DNA binding properties

DNA is the primary pharmacological target of antitumor drugs and therefore, it is essential to explore the interactions of metal complexes with DNA for the development of effective chemotherapeutic agents. Particularly, metal complexes in a well-tailored ligand framework are responsible for specific shape and surface features that complement the molecular target site usually major/minor groove of the DNA double helix and metal complex-DNA interactions are therefore, of paramount importance. The mode and propensity of binding of the metal complexes to CT-DNA were examined by using emission spectra.

#### 3.6.1. Fluorescence spectral studies

Fluorescence emission spectroscopy is an effective method to examine the binding mode and binding extent of metal complexes with DNA. In general, hypochromism and red-shift are associated with the intercalation of the metal complexes to the DNA helix, due to the intercalative mode involving a strong stacking interaction between the aromatic chromophore of the metal complexes and the base pairs of DNA [40]. The emission spectra of the two cobalt(III) complexes in the absence and presence of CT-DNA are given in Fig. 4. It can be seen from this figure, when titrated by CT-DNA, the emission bands of complexes **1** and **2** at 428 and 414 nm exhibit hypochromism of about 20.12% and 18.36% with slightly red shifts of 3 nm. The marked decreases in the fluorescence intensity of the new complexes indicate the intercalative binding mode of DNA. In order to quantitatively investigate the binding affinity of the cobalt(III) complexes toward CT-DNA, the intrinsic binding constants  $K_b$  were determined by monitoring the changes in emissions at 428 and 414 nm for complexes **1** and **2** using the following equation Scatchard equation.

$$C_F = C_T [(I/I_0) - P] / [1 - P]$$

where,  $C_T$  is concentration of the probe (complex) added,  $C_F$  is the concentration of the free probe, and  $I_0$  and  $I$  are its emission intensities in the absence and in the presence of DNA, respectively.  $P$  is the ratio of the observed emission quantum yield of the bound probe to the free probe. The value of  $P$  was obtained from a plot of  $I/I_0$  versus  $1/[DNA]$  such that the limiting emission yield is given by the y-Intercept. The amount of bound probe ( $C_B$ ) at any concentration was equal to  $C_T - C_F$ . The scatchard plots of  $r/C_F$  versus  $r$  for complexes **1** and **2** with increasing concentration of CT-DNA shown in Fig. S15 (Supporting information). A plot of  $r/C_F$  versus  $r (= C_B/[DNA])$  gave the binding isotherm and the best fit of the data resulted in the intrinsic binding constant ( $K_b$ ) values was calculated from the ratio of slope and the intercept [41]. The  $K$  (emission binding constant) values are  $1.69 \times 10^5 \text{ M}^{-1}$  and  $1.76 \times 10^5 \text{ M}^{-1}$

<sup>1</sup> for complexes **1** and **2**. These results revealed that the complexes bind to DNA via intercalation mode. The order of the binding constants is **2** > **1**, indicates that **2** is showing stronger binding ability due to having N(4)-substitution of thiosemicarbazone for phenyl enhances DNA binding affinity. The interaction of phenyl with DNA is favoured by the larger extension of the aromatic moiety. This result is in accordance with other works on cobalt complexes containing phenylthiosemicarbazone [42].

<Insert Figure 4>

### 3.6.2. Competitive studies with methylene blue

DNA binding study point out that the new cobalt(III) complexes effectively bind to DNA. Further, this has been confirmed by methylene blue (MB) displacement experiments. In general, the intrinsic fluorescence intensity of DNA is very low, and that of MB in Tris-HCl buffer is also not high due to quenching by the solvent molecules. However, on addition of DNA to MB, the fluorescence intensity of MB will be enhanced because of its intercalation into the DNA. Thus, MB can be used to probe the interaction of complexes with DNA. The fluorescence intensity of MB can be quenched by the addition of second DNA binding molecule by either replacing the MB and/or by accepting the excited-state electron of the MB through a photoelectron transfer mechanism. The fluorescence spectra of MB were measured using an excitation wavelength of 605 nm, and the emission range was set between 630 and 850 nm. The fluorescence quenching spectra of DNA-bound MB for complexes **1** and **2** were shown in Fig. S16 (Supporting information). This illustrate that, as the concentration of the complexes increases, the emission band at 684 nm exhibited hypochromism up to 51.69% and 76.24% of the initial fluorescence intensity. The observed decrease in the fluorescence intensity clearly indicates that the MB molecules are displaced from their DNA binding sites and are replaced by the complexes under investigation [43]. Quenching data were analyzed according to the following Stern-Volmer equation:

$$F_0/F = K_q [Q] + 1$$

where  $F_0$  is the emission intensity in the absence of complex,  $F$  is the emission intensity in the presence of complex,  $K_q$  is the quenching constant, and  $[Q]$  is the concentration of the complex. The  $K_q$  value is obtained as a slope from the plot of  $F_0/F$  versus  $[Q]$ . In the Stern-Volmer plot (Fig. S17, Supporting information) of  $F_0/F$  versus  $[Q]$ , the quenching constant ( $K_q$ ) is obtained from the slope which was  $1.4 \times 10^4 \text{ M}^{-1}$  and  $4.30 \times 10^4 \text{ M}^{-1}$  for the complexes **1** and **2** respectively. Further the apparent DNA binding constant ( $K_{app}$ ) were calculated using the following equation,

$$K_{MB} [MB] = K_{app} [\text{complex}]$$

(where the complex concentration has the value at a 50% reduction of the fluorescence intensity of MB,  $K_{MB}$  ( $1.0 \times 10^{-7} \text{ M}^{-1}$ ) is the DNA binding constant of MB to DNA,  $[MB] = 7.5 \text{ } \mu\text{M}$ ), where found to be  $1.05 \times 10^6 \text{ M}^{-1}$  and  $3.2 \times 10^6 \text{ M}^{-1}$  respectively for **1** and **2**. The experimental results data again suggest that the complexes bind to DNA via intercalation, but the highest value of complex **2** suggesting its stronger ability to displace MB from the MB-DNA system.

### 3.7. DNA cleavage activity

Since cobalt(III) complexes showed good binding propensity with CT DNA, therefore the DNA cleavage activity of complexes was evaluated by agarose gel electrophoresis using supercoiled pBR322 plasmid DNA in a medium of 10 mM Tris acetate/10 mM EDTA buffer solution (pH 8.0). The reaction mixture was subjected to agarose gel electrophoresis with increasing complex concentrations incubated at 310 K for 30 min. The activity of complexes was assessed by the conversion of DNA from Form I (Supercoiled Form) to Form II (Nicked Circular Form) and then to Form III (Linear Form). As shown in Fig. 5, it was observed that the complexes was found to exhibits nuclease activity at different concentration (10, 25 & 50  $\mu\text{g/mL}$ ), followed by conversion of supercoiled DNA (Form I) into NC DNA (Form II) without concurrent formation of Form III, suggesting single strand DNA cleavage. When the concentration was increased from 10  $\mu\text{g/mL}$  to 50  $\mu\text{g/mL}$ , the production of NC form of DNA was also increased. The figure shows that the complex **2** exhibits higher cleavage activity than the complex **1**.

<Insert Figure 5>

### 3.8. BSA binding studies

Serum albumin (SA) is the most abundant protein in plasma and is capable of binding, transporting and delivering an extraordinarily diverse range of endogenous and exogenous compounds like fatty acids, nutrients, steroids, certain metal ions, hormones and a variety of therapeutic drugs [44-46] in the blood stream to their target organs [47]. Because of its structural homology with human serum albumin (HSA), bovine serum albumin (BSA) has been most extensively studied. Binding to these proteins may lead to loss or enhancement of the biological properties of the original drug, or provide paths for drug transportation. In order to get more information on the binding of the complexes with BSA, fluorescence

spectrum of BSA was studied upon the addition of the complexes. Though BSA contains three fluorophores, namely, tryptophan, tyrosine, and phenylalanine, the intrinsic fluorescence of BSA is mainly due to tryptophan alone, because phenylalanine has a very low quantum yield and the fluorescence of tyrosine is almost quenched when it becomes ionized or near to an amino group, a carbonyl group, or a tryptophan residue [48]. Changes in the emission spectra of tryptophan are common in response to protein conformational transitions, subunit associations, substrate binding, or denaturation. Hence, the interaction of BSA with cobalt complexes was studied by fluorescence measurement at room temperature. A solution of BSA (1  $\mu\text{M}$ ) was titrated with various concentrations of the complexes (0-50  $\mu\text{M}$ ) and fluorescence spectra were recorded in the range of 290 – 500 nm upon excitation at 280 nm. On increasing the concentration of complexes, a progressive decrease in the fluorescence intensity was observed, accompanied with a blue shift are shown in Fig. S18 (Supporting information).

It can be seen from Fig. S18, the fluorescence emission intensities of BSA at 344 nm show moderate decreasing trend with increasing concentration of the two complexes, up to 62.69% and 57.44% from the initial fluorescence intensity of BSA accompanied by a hypsochromic shift of 2 and 3 nm indicating that the interaction of the complexes with BSA could cause changes in protein secondary structure leading to changes in tryptophan environment of BSA [49].

Furthermore fluorescence quenching data were analyzed with the Stern–Volmer equation and Scatchard equation. From the plot of  $I_0/I$  versus  $[Q]$ , the quenching constant ( $K_q$ ) can be calculated using the plot of  $I_0/I$  versus  $[Q]$  (Fig. S19A, Supporting information). If it is assumed that the binding of complexes with BSA occurs at equilibrium, the equilibrium binding constant can be analyzed according to the Scatchard equation:

$$\log [(I_0 - I)/I] = \log K_{\text{bin}} + n \log [Q]$$

where  $K_{\text{bin}}$  is the binding constant of the compound with BSA and  $n$  is the number of binding sites. The number of binding sites ( $n$ ) and the binding constant ( $K_{\text{bin}}$ ) have been found from the plot of  $\log (I_0 - I)/I$  vs  $\log [Q]$  (Fig. S19B, Supporting information). The calculated  $K_q$ ,  $K_{\text{bin}}$ , and  $n$  values are given in Table 3. The values of  $K_q$  and  $K_{\text{bin}}$  suggested that the complex **2** interact with BSA more strongly than the complex **1** could be due to the presence of extended delocalization of electrons by the aromatic ring i.e., phenyl group substituted at the thiosemicarbazone which facilitate its BSA binding propensity as observed in the DNA binding experiments discussed in the previous section.

**Table 3**

Quenching constant ( $K_q$ ), binding constant ( $K_{bin}$ ), and number of binding sites ( $n$ ) for the interactions of complexes with BSA.

Complex	$K_q$ ( $M^{-1}$ )	$K_{bin}$ ( $M^{-1}$ )	N
<b>1</b>	$8.58 \times 10^4$	$1.12 \times 10^5$	1.52
<b>2</b>	$8.66 \times 10^4$	$1.27 \times 10^5$	1.60

### 3.9. Evaluation of radical scavenging ability

The free radicals play an important role in the inflammatory process. Many thiosemicarbazone derivatives with a broad spectrum have been reported to act either as inhibitors of free radical production or as radical scavengers [23,42, 50-54]. Thus, compounds with possible antioxidant properties could play a crucial role against inflammation and can lead to potentially effective drugs. Antioxidants which exhibit radical scavenging activity have been receiving increased attention since they show interesting anticancer, anti-aging and anti-inflammatory activities [52-57]. The radical scavenging activities of our compounds along with standards such as butylated hydroxytoluene (BHT) and Vitamin C in a cell free system have been examined with reference to DPPH radicals (DPPH), hydroxyl radicals (OH), and nitric oxide (NO) and their corresponding  $IC_{50}$  values have been tabulated in Table 4. The power of radical scavenging ability of the ligands and complexes were found to be higher than that of the standard antioxidants (Fig. S20, Supporting information). By comparing the antioxidant activity of the ligands and with that of the metal complexes it became clear that the metal complexes possess higher scavenging activity towards various free radicals than the respective parent ligands. The NO scavenging power of the tested complexes was found to be enhanced than that for the other radicals studied.

**Table 4**

Antioxidant activity of ligands, cobalt(III) complexes, BHT and vitamin C against various radicals.

Compound	IC <sub>50</sub> (μM)		
	DPPH	OH	NO
H <sub>3</sub> L <sup>1</sup> .Cl	65.32 ± 0.5	47.45 ± 0.3	33.92 ± 0.2
H <sub>3</sub> L <sup>2</sup> .Cl	61.21 ± 0.2	43.74 ± 0.4	32.29 ± 0.4
<b>1</b>	48.73 ± 0.3	39.83 ± 0.1	27.39 ± 0.2
<b>2</b>	45.27 ± 0.4	33.68 ± 0.6	26.53 ± 0.3
BHT	86.53 ± 0.6	163.80 ± 0.5	154.30 ± 0.8
Vitamin C	147.20 ± 0.8	232.20 ± 0.7	215.72 ± 0.9

### 3.10. Cytotoxic activity evaluation by MTT assay

The positive results obtained from DNA binding, DNA cleavage, protein binding and antioxidative studies of the new Co(III) pyridoxal N(4)-substituted thiosemicarbazone complexes encouraged us to test its cytotoxicity against a panel of human cancer cell lines. *In vitro* cytotoxicity of compounds was evaluated by means of the standard MTT-dye reduction assay which is a widely used method in biological evaluation. The cytotoxic activity of pyridoxal N(4)-substituted thiosemicarbazone ligands and their Co(III) complexes were tested against human breast carcinoma (MCF-7) and human cervix carcinoma (HeLa) tumor cell lines. Compounds were dissolved in DMSO and blank samples containing the same volume of DMSO were taken as controls to identify the activity of solvent in this cytotoxicity experiment. The exhibited IC<sub>50</sub> values (the concentration needed to inhibit 50% of the cellular proliferation) after 48 h of incubation are given in Table 5. The cell viability was concentration-dependent (1-100 μM), with increasing the concentrations a decrease in cell viability was observed (Fig. S21a-b, Supporting information).

**Table 5**

IC<sub>50</sub> (μM) value of cobalt(III) complexes and cisplatin against human breast carcinoma cell line (MCF-7) and human cervix carcinoma cell line (HeLa).

Compound	IC <sub>50</sub> (μM) <sup>a</sup>	
	MCF-7	HeLa
H <sub>3</sub> L <sup>1</sup> .Cl	>100	>100
H <sub>3</sub> L <sup>2</sup> .Cl	>100	>100
<b>1</b>	6.01±0.08	83.24± 1.03
<b>2</b>	1.00±0.09	20.28± 2.09
Cisplatin	3.19±0.02	53.50± 0.07

<sup>a</sup>Fifty percent inhibitory concentration after exposure for 48 h in the MTT assay.

The IC<sub>50</sub> value showed that the Co(III) complex exhibited significant activity against MCF-7 and HeLa cell lines. Interestingly, on comparing the IC<sub>50</sub> values of complex **2** with well-known anticancer drug cisplatin against MCF-7 and HeLa cell lines the inhibitory activity of the complex **2** is about two to three times higher than that of cisplatin. It was also observed that **1** and **2** demonstrated a noticeable cytotoxicity against all cell lines when compared with the free ligands, implying that the biological activity is largely ascribed by the presence of the Co(III) metal centre. In addition, complex **2** exhibited a slightly higher cytotoxicity than complex **1** against both cell lines. These results suggest that the terminal phenyl substitution of the ligand increased the cytotoxic activity of the complex **2** in these two cell lines, as observed in the screening of other previously reported antitumor agents containing phenyl substitution [58,59]. Furthermore, a comparison of the biological activities of new complexes with that of our previously reported cobalt complexes with other ligands has revealed that the complex **2** exhibits superior activity [23d].

#### 4. Conclusions

Two new trivalent cobalt complexes with pyridoxal N(4)-substituted thisemicarbazone ligands have been synthesized and well characterized in detailed by elemental analysis and spectral techniques (IR, electronic, <sup>1</sup>H NMR and ESI-Mass). The molecular structure of the complex **2** investigated through X-ray crystallography demonstrated distorted octahedral geometry around the metal ion with two ligand molecules. From the X-ray analysis, it was found that in complex **2**, the two ligands coordinated as a dibasic tridentate donor by forming a stable pairs of five-membered and six-membered rings through phenolic oxygen, azomethine nitrogen, and thiolate sulfur atoms. The new complexes were subjected to studies

of their potential biological properties such as DNA binding/cleavage, protein binding, antioxidant and cytotoxicity. The DNA interaction of the complexes has been evaluated by fluorescence spectroscopy which revealed that both complexes can bind to DNA via intercalation. The experimental results suggested that the complex **2** can bind to DNA more strongly than the complex **1** due to phenyl substitution in thiosemicarbazone. Both the complexes cleaved plasmid pBR322 DNA through gel electrophoresis assay. The protein binding properties of the complexes examined by the fluorescence spectra suggested that the binding affinity increases in the phenyl substitution at the terminal nitrogen of the thiosemicarbazone moiety. In addition, the complexes also exhibited excellent radical scavenging activities over the ligands, and standard antioxidants. The cytotoxicity of the complexes in MTT assay showed that the complexes exhibited higher activity than their parent ligands and the predictable standard cisplatin in both cell lines used for the investigation. Correlating the activity of the complexes with their substitution of thiosemicarbazone, we found that the substitution of the phenyl ring at the thiosemicarbazone of the ligand increases the degree of cytotoxicity.

### **Acknowledgements**

We are thankful to the IISC Bangalore, STIC Cochin, SAIF Panjab University, Chandigarh, KMCH Coimbatore and Biogenics Hubli, India for providing instrumental facilities. The author (R. N) thankful to DST for financial assistant in the form project (No.SR/FT/CS-95/2010).

### **Supplementary material**

CCDC 977570 contains the supplementary crystallographic data for the complex  $[\text{Co}(\text{HL}^3\cdot\text{Cl})(\text{HL}^3\cdot\text{H}_2\text{O})]$ . These data can be obtained free of charge via <http://www.ccdc.cam.ac.uk/conts/retrieving.html>, or from the Cambridge Crystallographic Data Centre, 12 Union Road, Cambridge CB2 1EZ, UK; fax: (+44) 1223-336-033; or e-mail: [deposit@ccdc.cam.ac.uk](mailto:deposit@ccdc.cam.ac.uk).

### **References**

- [1] M. Belicchi Ferrari, F. Bisceglie, E. Leporati, G. Pelosi, P. Tarasconi, *Bull. Chem. Soc. Jpn.* 75 (2002) 781–782.
- [2] M. Belicchi Ferrari, F. Bisceglie, G. Pelosi, P. Tarasconi, R. Albertini, P. P. Dall'Aglio, S. Pinelli, A. Bergamo, G. Sava, *J. Inorg. Biochem.* 98 (2004) 301–312.
- [3] (a) M. Belicchi Ferrari, G. Fava Gasparri, E. Leoparti, C. Pelizzi, P. Tarasconi, G. Tosi, *J. Chem. Soc., Dalton Trans.* (1986) 2455–2461; (b) M. Belicchi Ferrari, G. Gasparri Fava, C. Pelizzi, P. Tarasconi, G. Tosi, *J. Chem. Soc., Dalton Trans.* (1987) 227–233; (c) M. Belicchi Ferrari, G. Gasparri Fava, M. Lanfranchi, C. Pelizzi, P. Tarasconi, *J. Chem. Soc., Dalton Trans.* (1991) 1951–1957; (d) M. Belicchi Ferrari, G. Gasparri Fava, G. Pelosi, M.C. Rodriguez-Argüelles, P. Tarasconi, *J. Chem. Soc., Dalton Trans.* (1995) 3035–3040; (e) M. Belicchi Ferrari, G. Gasparri Fava, C. Pelizzi, P. Tarasconi, G. Tosi, *Rev. Port. Quim.* 27 (1985) 328; (f) M. Belicchi Ferrari, G. Gasparri Fava, P. Tarasconi, C. Pelizzi, XVIII Congresso Nazionale, Associazione Italiana di Cristallografia, Como, 1987, p. 89; (g) M. Belicchi Ferrari, G. Gasparri Fava, S. Pinelli, P. Tarasconi, C. Pelizzi, Congresso Interdivisionale della Società Chimica Italiana, Perugia, 1989, p. 405; (h) V. M. Leovac, L. S. Jovanovic, V. Divjakovic, A. Pevec, I. Leban, T. Armbruster, *Polyhedron* 26 (2007) 49–58; (i) V. M. Leovac, L. S. Jovanovic, V. S. Jevtovic, G. Pelosi, F. Bisceglie, *Polyhedron* 26 (2007) 2971–2978; (j) J. Pisk, B. Prugovecki, D. Matkovic-Calogovic, R. Poli, D. Agustin, V. Vrdoljak, *Polyhedron* 33 (2012) 441–449; (k) E. W. Yemeli Tido, C. Faulmann, R. Roswanda, A. Meetsma, P. J. van Koningsbruggen, *Dalton Trans.* 39 (2010) 1643–1651.
- [4] V. M. Leovac, V. S. Jevtovic, G. A. Bogdanovic, *Acta Crystallogr., Sect. C* 58 (2002) m514–m516.
- [5] U. Abram, K. Ortner, R. Gust, K. Sommer, *J. Chem. Soc., Dalton Trans.* (2000) 735–744.
- [6] J. S. Casas, E. E. Castellano, M. C. Rodríguez-Argüelles, A. Sánchez, J. Sordo, J. Zukerman, *Inorg. Chim. Acta* 260 (1997) 183–188.
- [7] P. V. Bernhardt, G. A. Lawrance, in: J. A. McCleverty, T. J. Meyer (Eds.), *Comprehensive Coordination Chemistry II*, vol. 6 (2003) pp. 1–45 ch. 1.
- [8] P. J. Sadler, *Adv. Inorg. Chem.* 36 (1991) 1–48.
- [9] M. D. Hall, T. W. Failes, N. Yamamoto, T. W. Hambley, *Dalton Trans.* (2007) 3983–3990.
- [10] N. Hadjiladis, E. Sletten (Eds.), *Metal Complex e DNA Interactions*, John Wiley &

- Sons, Inc., Hoboken, NJ, 2009 and the references therein.
- [11] H. Lopez-Sandoval, M. E. Londono-Lemos, R. Garza-Velasco, I. Poblano-Melendez, P. Granada-Macias, I. Gracia-Mora, N. Barba-Behrens, *J. Inorg. Biochem.* 102 (2008) 1267–1276.
- [12] I. Ott, A. Abraham, P. Schumacher, H. Shorafa, G. Gastl, R. Gust, B. Kircher, *J. Inorg. Biochem.* 100 (2006) 1903–1906.
- [13] R. Eshkourfu, B. Cobeljic, M. Vujcic, I. Turel, A. Pevec, K. Sepcic, M. Zec, S. Radulovic, T. Srdic-Radic, D. Mitic, K. Andjelkovic, D. Sladic, *J. Inorg. Biochem.* 105 (2011) 1196–1203.
- [14] D. U. Miodragovic, G. A. Bogdanovic, Z. M. Miodragovic, M. D. Radulovic, S. B. Novakovic, G. N. Kaludjerovic, H. Kozlowski, *J. Inorg. Biochem.* 100 (2006) 1568–1574.
- [15] K. Nomiya, A. Yoshizawa, K. Tsukagoshi, N. C. Kasuga, S. Hirakawa, J. Watanabe, *J. Inorg. Biochem.* 98 (2004) 46–60.
- [16] E. K. Efthimiadou, A. Karaliota, G. Psomas, *Bioorg. Med. Chem. Lett.* 18 (2008) 4033–4037.
- [17] J. Lv, T. Liu, S. Cai, X. Wang, L. Liu, Y. Wang, *J. Inorg. Biochem.* 100 (2006) 1888–1896.
- [18] Z. Weiqun, Y. Wen, X. Liqun, C. Xianchen, *J. Inorg. Biochem.* 99 (2005) 1314–1319.
- [19] A. Bottcher, T. Takeuchi, K. I. Hardcastle, T. J. Meade, H. B. Gray, *Inorg. Chem.* 36 (1997) 2498–2504.
- [20] T. Takeuchi, A. Bottcher, C.M. Quezada, T.J. Meade, H.B. Gray, *Bioorg. Med. Chem.* 7 (1999) 815–819.
- [21] F. Dimiza, A. N. Papadopoulos, V. Tangoulis, V. Psycharis, C.P. Raptopoulou, D. P. Kessissoglou, G. Psomas, *Dalton Trans.* 39 (2010) 4517–4528.
- [22] F. Dimiza, A. N. Papadopoulos, V. Tangoulis, V. Psycharis, C. P. Raptopoulou, D. P. Kessissoglou, G. Psomas, *J. Inorg. Biochem.* 107 (2012) 54–64.
- [23] (a) R. Manikandan, N. Chitrapriya, Y. J. Jang, P. Viswanathamurthi, *RSC Adv.* 3 (2013) 11647–11657; (b) P. Anitha, N. Chitrapriya, Y. J. Jang, P. Viswanathamurthi, *J. Photochem. Photobiol. B* 129 (2013) 17–26; (c) S. Selvamurugan, R. Ramachandran, P. Viswanathamurthi, *Biometals*, DOI 10.1007/s10534-013-9649-8; (d) R. Manikandan P. Viswanathamurthi, K. Velmurugan, R. Nandhakumar, T. Hashimoto, A. Endo, *J. Photochem. Photobiol. B* 130 (2014) 205–216.
- [24] G. N. Rao, Ch. Janardhana, K. Pasupathy, P. Mahesh Kumar, *Ind. J. Chem.* 39B (2000)

- 151–153.
- [25] E. W. Yemeli Tido, E. J. M. Vertelman, A. Meetsma, P. J. van Koningsbruggen, *Inorg. Chim. Acta* 360 (2007) 3896–3902.
- [26] G. M. Sheldrick, *Acta Crystallogr. Sect. A* 46 (1990) 467–473.
- [27] G. M. Sheldrick, *SHELXL-97: FORTRAN Program for Crystal Structure Refinement*, Göttingen University, 1997.
- [28] J. Sambrook, E. F. Fritsch, T. Maniatis, *Molecular cloning, A laboratory Manual*. 2nd Edn. Cold Spring, Harbor Laboratory, Cold Spring Harbor, New York, 1989.
- [29] M. S. Blois, *Nature* 29 (1958) 1199–1200.
- [30] T. Nash, *Biochem. J.* 55 (1953) 416–421.
- [31] L. C. Green, D. A. Wagner, J. Glogowski, P. L. Skipper, J. S. Wishnok, R. Tannenbaum, *Anal. Biochem.* 126 (1982) 131–138.
- [32] M. Blagosklong, W. S. EI-diery, *Int. J. Cancer* 67 (1996) 386–392.
- [33] L. S. Vojinovic, V. M. Leovac, S. B. Novakovic, G. A. Bogdanovic, J. J. Csanadi, V. I. Cesljevic, *Inorg. Chem. Commun.* 7 (2004) 1264–1268.
- [34] M. Mohan, N. S. Gupta, M. Kumar, *Trans. Met. Chem.* 19 (1994) 265–269.
- [35] A. Sreekanth, S. Sivakumar, M. R. Prathapachandra Kurup, *J. Mol. Struct.* 655 (2003) 47–58.
- [36] B. Shaabani, A. A. Khandar, F. Mahmoudi, S. S. Balula, L. Cunha-Silva, *J. Mol. Struct.* 1045 (2013) 55–61.
- [37] V. Vrdoljak, J. Pisk, B. Prugovecki, D. Matkovic-Calogovic, *Inorg. Chim. Acta* 362 (2009) 4059–4064.
- [38] S. S. Massoud, F. A. Mautner, M. Abu-Youssef, N.M. Shuaib, *Polyhedron* 18 (1999) 2287–2291.
- [39] S. Sasi, M. R. Prathapachandra Kurup, E. Suresh, *J. Chem. Crystallogr.* 37 (2007) 31–36.
- [40] T. Sathiya Kamatchi, N. Chitrapriya, H. Lee, C. F. Fronczek, F. R. Fronczek, K. Natarajan, *Dalton Trans.* 41 (2012) 2066–2077.
- [41] S. Satyanarayana, J. C. Dabrowiak, J. B. Chaires, *Biochemistry* 31 (1992) 9319–9324.
- [42] E. Ramachandran, S. P. Thomas, P. Poornima, P. Kalaivani, R. Prabhakaran, V. Vijaya Padma, K. Natarajan, *Eur. J. Med. Chem.* 50 (2012) 405–415.
- [43] N. Shahabadi, M. Falsafi, N. H. Moghadam, *J. Photochem. Photobiol. B* 122 (2013) 45–51.

- [44] K. Yamasaki, T. Maruyama, U. Kragh-Hansen, M. Otagiri, *Biochim. Biophys. Acta* 1295 (1996) 147–157.
- [45] X. M. He, D. C. Carter, *Nature* 358 (1992) 209–215.
- [46] I. Sjöholm, B. Ekman, A. Kober, I. Ljungstedt-Pahlman, B. Seiving, T. Sjödin, *Mol. Pharmacol.* 16 (1979) 767–777.
- [47] N. Ibrahim, H. Ibrahim, S. Kim, J. P. Nallet, F. O. Nepveu, *Biomacromolecules* 11 (2010) 3341–3351.
- [48] A. Sulowska, *J. Mol. Struct.* 614 (2002) 227–232.
- [49] S. S. Bhat, A. A. Kumbhar, H. Heptullah, A. A. Khan, V. V. Gobre, S. P. Gejji, V. G. Puranik, *Inorg. Chem.* 50 (2011) 545–558.
- [50] Z. C. Liu, B. D. Wang, Z. Y. Yang, Y. Li, D. D. Qin, T. R. Li, *Eur. J. Med. Chem.* 44 (2009) 4477–4484.
- [51] D. Senthil Raja, G. Paramaguru, N. S. P. Bhuvanesh, J. H. Reibenspies, R. Renganathan, K. Natarajan, *Dalton Trans.* 40 (2011) 4548–4559.
- [52] D. Senthil Raja, N. S. P. Bhuvanesh, K. Natarajan, *Eur. J. Med. Chem.* 46 (2011) 4584–4594.
- [53] E. Ramachandran, D. Senthil Raja, N. P. Rath, K. Natarajan, *Inorg. Chem.* 52 (2013) 1504–1514.
- [54] R. Prabhakaran, P. Kalaivani, R. Huang, P. Poornima, V. Vijaya Padma, F. Dallemer, K. Natarajan, *J. Biol. Inorg. Chem.* 18 (2013) 233–247.
- [55] D. Senthil Raja, N. S. P. Bhuvanesh, K. Natarajan, *J. Biol. Inorg. Chem.* 17 (2012) 223–237.
- [56] D. Senthil Raja, N. S. P. Bhuvanesh, K. Natarajan, *Inorg. Chim. Acta* 385 (2012) 81–93.
- [57] C. Kontogiorgis, D. Hadjipavlou-Litina, *J. Enzyme Inhib. Med. Chem.* 18 (2003) 63–69.
- [58] E. Ramachandran, D. Senthil Raja, a N. S. P. Bhuvanesh, K. Natarajan, *Dalton Trans.* 41 (2012) 13308–13323.
- [59] E. Ramachandran, D. Senthil Raja, J. L. Mike, T. R. Wagner, M. Zeller, K. Natarajan, *RSC Adv.* 2 (2012) 8515–8525.

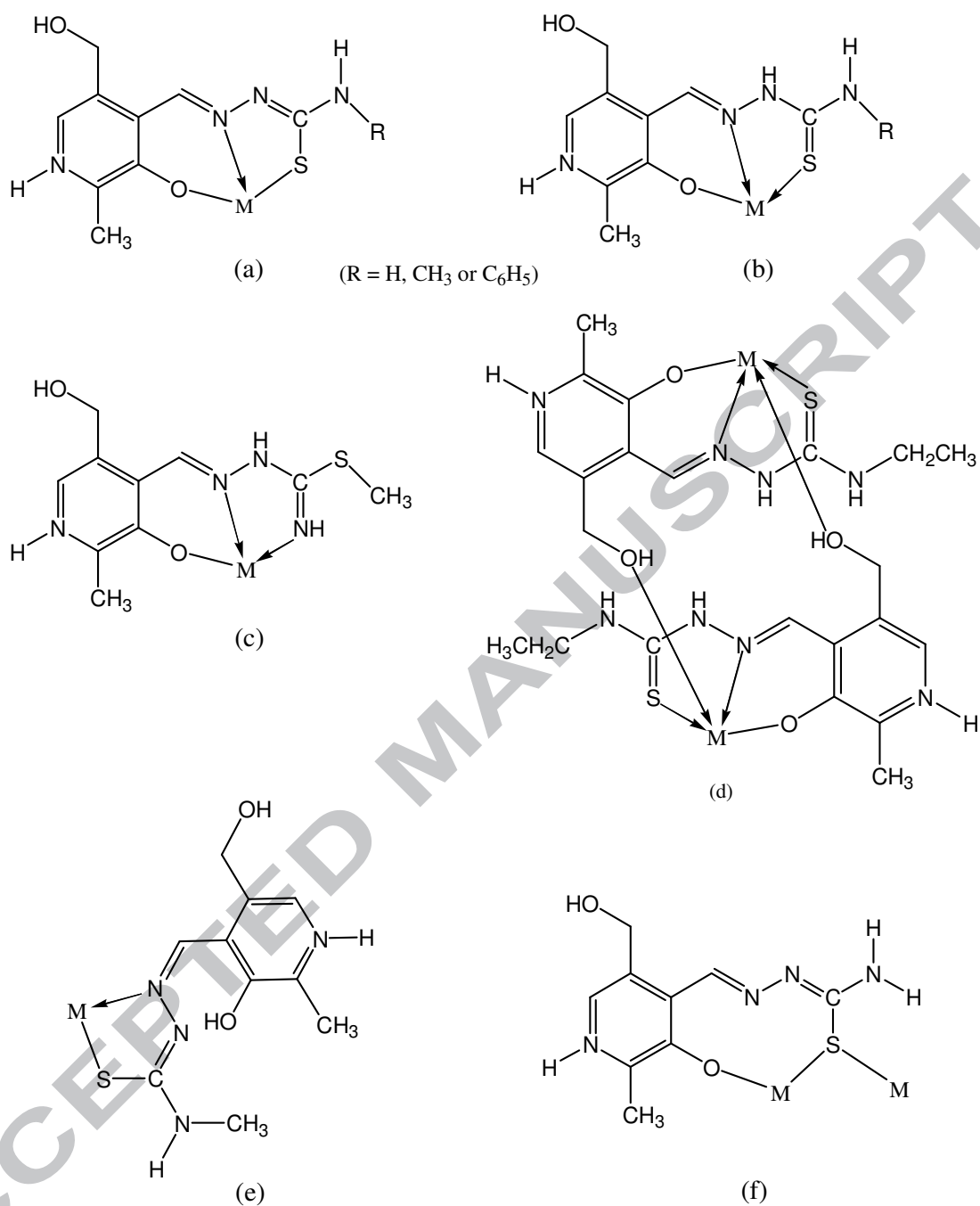
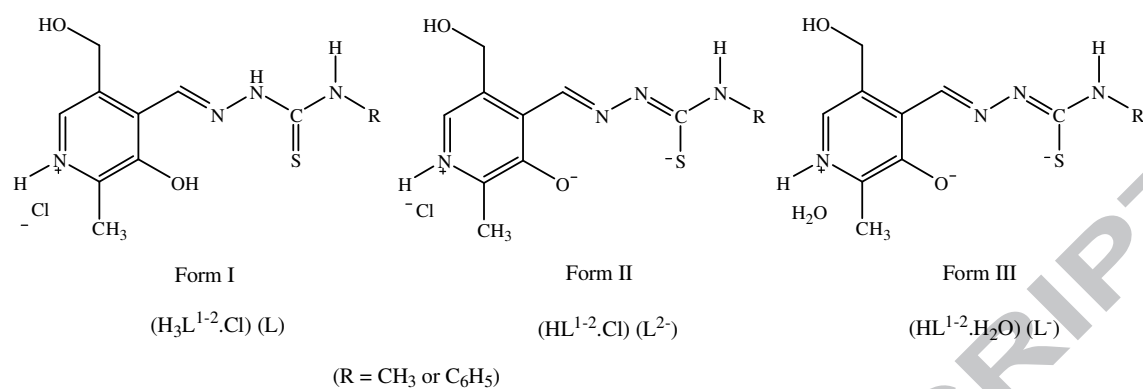
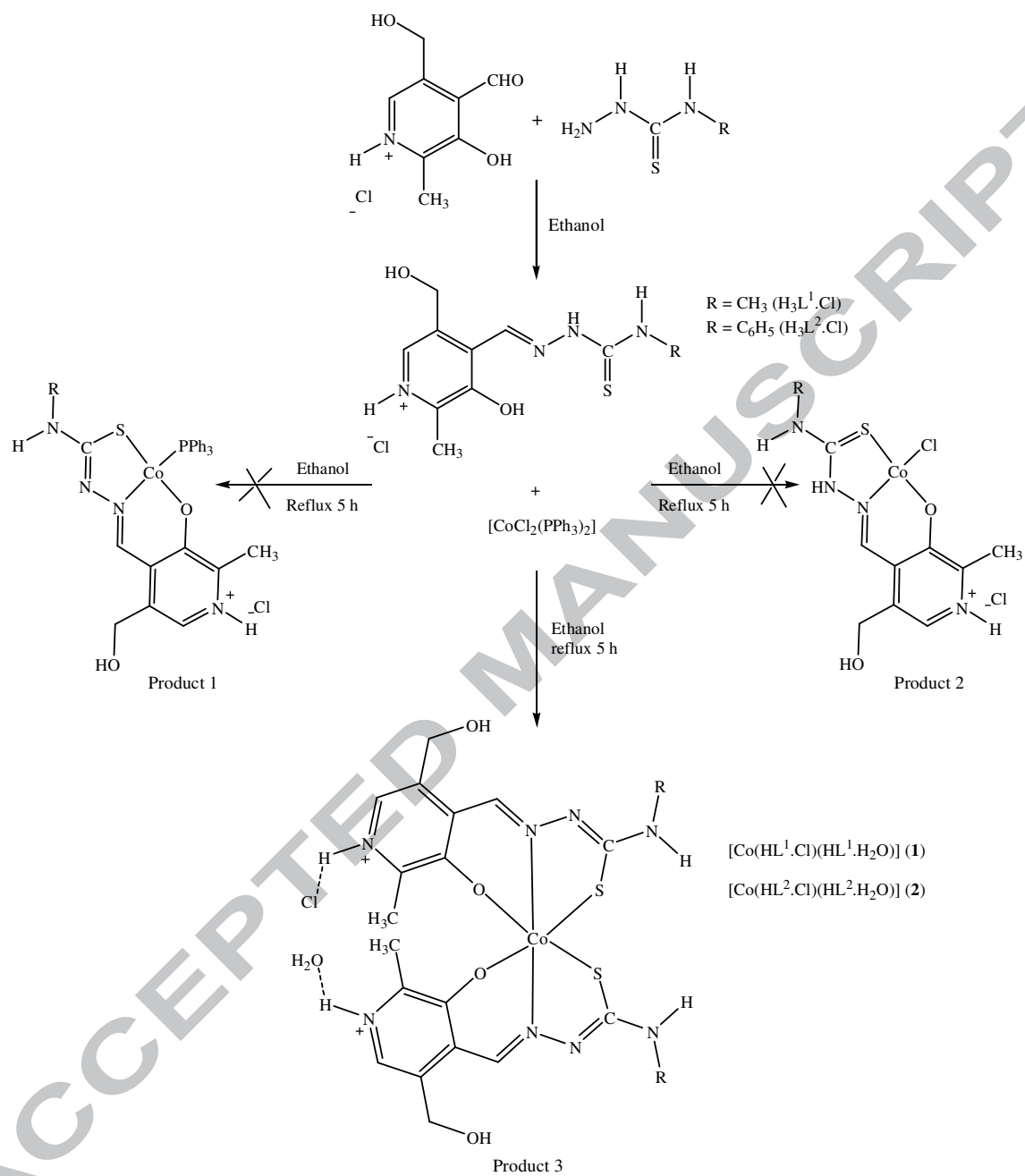


**Fig. 1.** Modes of binding in pyridoxal thiosemicarbazone ligands.



**Scheme 1.** Pyridaxol N(4)-substituted thiosemicarbazone ligand modulation.



**Scheme 2.** Synthesis of Co(III) pyridaxol N(4)-substituted thiosemicarbazone complexes.

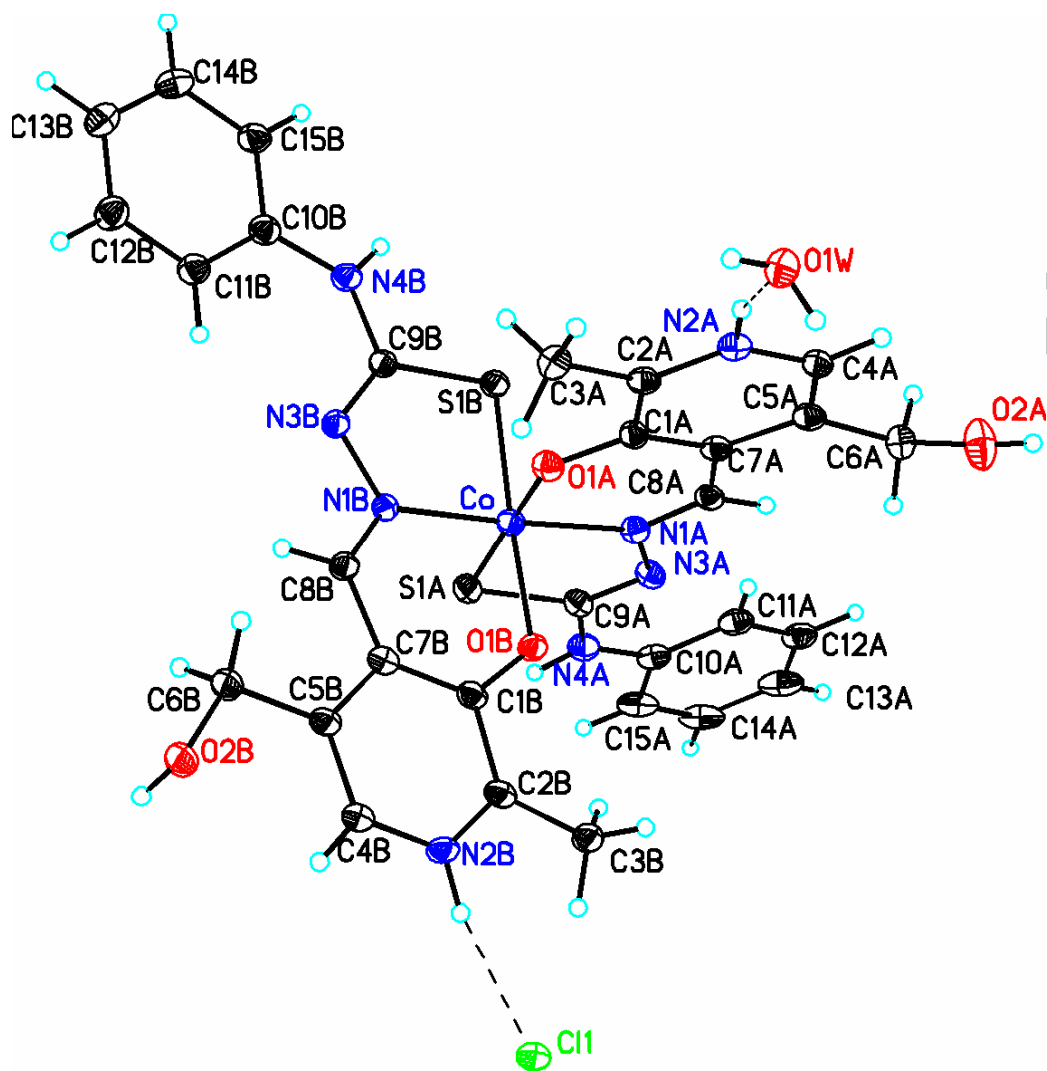
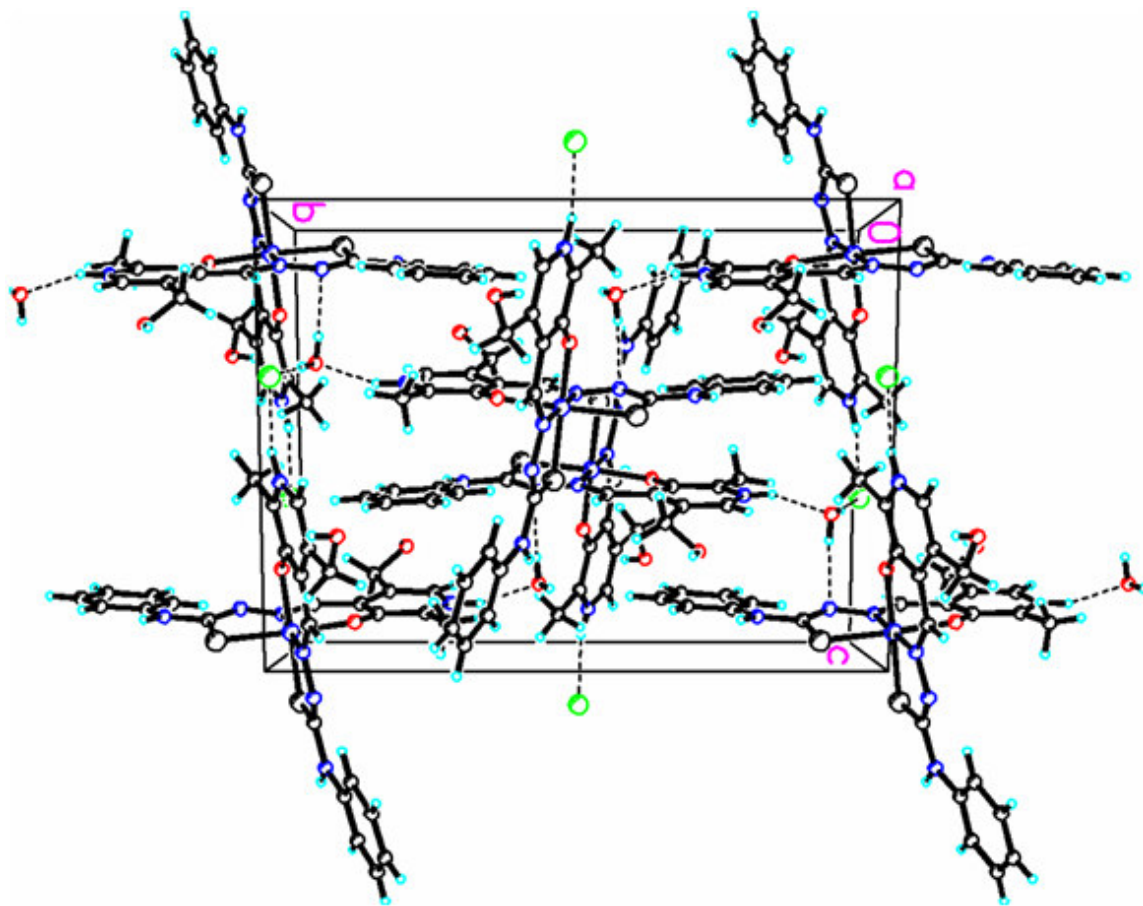
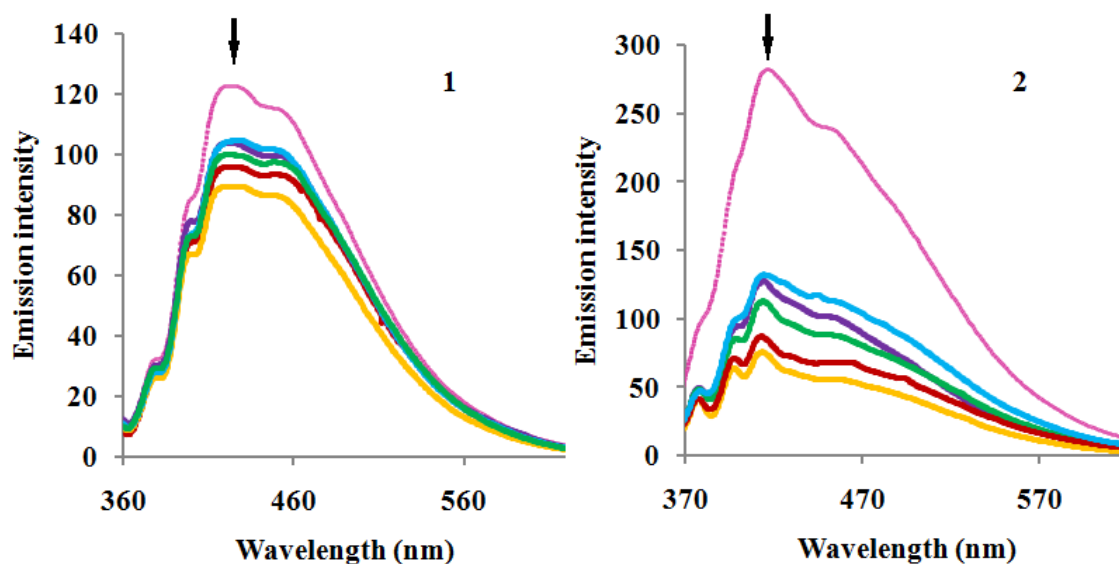


Fig. 2. ORTEP view of complex 2.



**Fig. 3.** Crystal packing diagram for complex 2.



**Fig. 4.** Fluorescence spectra of cobalt(III) complexes **1-2** ( $25 \mu\text{M}$ ,  $\lambda_{\text{exi}} = 400 \text{ nm}$ ) in  $5 \text{ mM}$  Tris-HCl/ $50 \text{ mM}$  NaCl buffer at pH 7.2 and arrows indicate absence and presence of increasing amounts of CT-DNA concentration ( $0, 5, 10, 15, 20, 25 \mu\text{M}$ ) at  $25 \text{ }^\circ\text{C}$ .

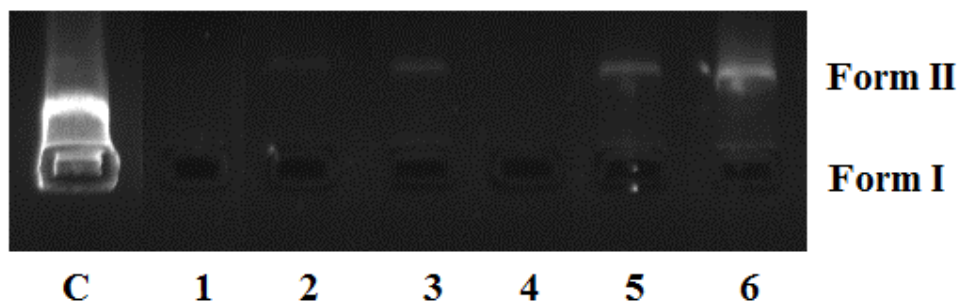
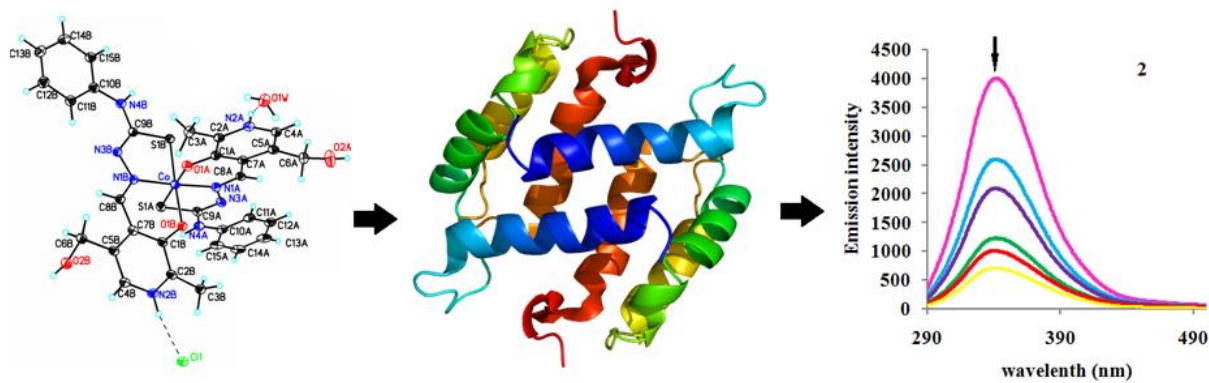


**Fig. 5.** Agarose gel electrophoresis diagram showing the cleavage of pBR322 DNA by Co(III) Schiff base complex in TAE Buffer (4.84 g Tris base, pH = 8, 0.5 M EDTA/1 L). Lane C, Control DNA (untreated complex); Lanes 1-3, in the different concentrations of complex **1**: (1) 10; (2) 25; (3) 50  $\mu\text{g/mL}$ ; Lanes 4-6, in the different concentrations of complex **2**: (1) 10; (2) 25; (3) 50  $\mu\text{g/mL}$ .



ACCEPTED MANUSCRIPT

## Synthesis, structure and *in vitro* biological activity of pyridoxal N(4)-substituted thiosemicarbazone cobalt(III) complexes

Rajendran Manikandan<sup>a</sup>, Paranthaman Vijayan<sup>a</sup>, Panneerselvam Anitha<sup>a</sup>, Govindan Prakash<sup>a</sup>, Periasamy Viswanathamurthi<sup>a,\*</sup>, Ray Jay Butcher<sup>b</sup>, Krishnaswamy Velmurugan<sup>c</sup>, Raju Nandhakumar<sup>c</sup>

<sup>a</sup>*Department of Chemistry, Periyar University, Salem-636011, Tamil Nadu, India.*

<sup>b</sup>*Department of Chemistry, Howard University, 525 College Street NW, Washington, DC 20059, USA.*

<sup>c</sup>*Department of Chemistry, Karunya University, Karunya Nagar, Coimbatore - 641 114, India.*

Cobalt(III) pyridoxal N(4)-substituted thiosemicarbazone complexes were synthesized and characterized. Crystal structure has been determined by X-ray diffraction. Their DNA/protein binding, DNA photocleavage, antioxidant and cytotoxic properties were studied.

### Highlights

- Cobalt(III) complexes bearing pyridoxal thiosemicarbazone were synthesized.
- One of the complexes **2** was characterized crystallographically.
- The complexes exhibited intercalation binding ability on DNA/BSA.
- The synthesized complexes showed good antioxidant activities.
- Complex **2** possesses higher cytotoxic activity.

ACCEPTED MANUSCRIPT